

## VENTILATION AND HEAT TRANSFER IN A SYMMETRICALLY VENTILATED SALIENT POLE SYNCHRONOUS MACHINE

S J Pickering, D Lampard, M Shanel

University of Nottingham, UK

### ABSTRACT

The results of a continuing effort to broaden understanding of heat transfer and ventilation in large synchronous salient pole electrical machines are presented. Heat transfer coefficients measured on an experimental four pole rotor for selected operational parameters are given and compared to Computational Fluid Dynamics (CFD) predictions. The experimental programme was carried out on a hydraulically smooth rotor and corresponding heat transfer coefficients measured for the purpose of CFD validation are presented. The effects of surface roughness on the predicted values of heat transfer coefficients are then considered. Particular attention is given to the field coil faces where "strip-on-edge" windings are extended to give a ribbed surface. A method using an equivalent roughness, to account for the enhanced heat transfer, without increasing demands for mesh density is explained.

The data presented demonstrate clearly the link between the flow field and the heat transfer coefficient. The potential use of CFD as a design tool to examine the effects of operating parameters and geometric modifications on heat transfer is illustrated.

### INTRODUCTION

The demand for increased efficiency and operational reliability of electrical machines requires special attention to the overall thermal management. In the case of large air-cooled salient pole machines the optimisation of the air flow path is a possible way to control the temperature distribution in the windings.

The airflow around a salient pole rotor, where heat is predominantly dissipated from the field coils by forced convection, dictates the intensity of cooling. The distribution of the heat transfer coefficients is complex, generally dependent on relative air velocity and locally determined by geometrical features. Some basic features of the heat transfer coefficient pattern are known, such as the difference between the leading and trailing sides of the pole or decrease in heat transfer coefficient along the rotor axis as the flow decelerates. Intensification of the heat transfer is often achieved by increasing the surface area directly subjected to the airflow, typically using ribs or fins.

It is within the capabilities of the latest commercial CFD codes to mesh and solve geometrically complicated flow regions in electrical machines (1). However, the finest geometrical details usually need to be eliminated to overcome meshing difficulties and

computational constraints. Also, assumptions of symmetry or periodicity may be needed to accommodate the whole machine within the computational limits. The accuracy of the analysis relies on empirical models, such as those for turbulence, rotation modelling or surface roughness.

### EXPERIMENTAL FACILITY

The authors have previously described the experimental validation of CFD modelling for a 1MVA synchronous four-pole machine with single-ended ventilation (2). The same experimental facility was adapted to simulate symmetric double-ended ventilation (Fig. 1). The rotor investigated was 464 mm in diameter and the rotor-stator air gap was 6 mm. Symmetrical ventilation was simulated by blocking the inter-polar spaces and the rotor-stator gap with baffles at an axial distance of 385 mm from the edge of the rotor core on a model ventilated from one end only.

After the entry to the end region, the air divided into two major streams – the first penetrating through the stator end windings towards an outlet between the first stator packet and stator end plate, and the second into the rotor inter-polar spaces and the rotor-stator gap to cool the rotor. This portion of flow gradually lost the axial component of its velocity on its way towards the symmetry plane as the air escaped through six stator radial ducts.

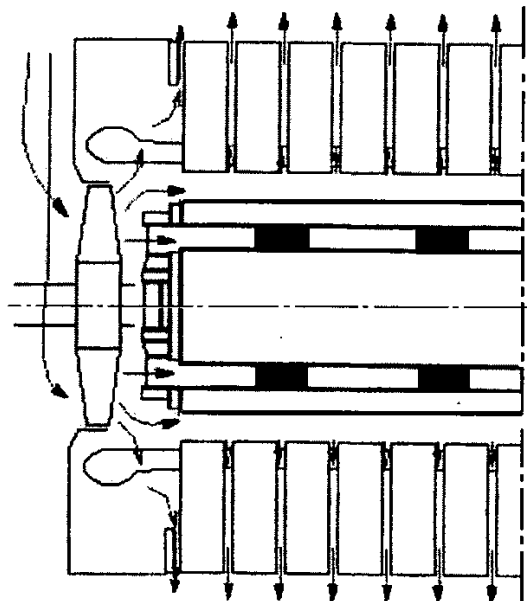


Fig. 1: Diagram of the double-ended ventilation scheme simulated in the investigation

A further modification to the rotor was the inclusion of the coil-supporting V-blocks in the inter-polar spaces. Several designs of V-block are in use in existing salient pole machines. Some act not only as a mechanical support to the field coils but may as well be built of conducting material to form some sort of a heat sink. The perception is that whatever their shape, the V-blocks affect the flow field in salient pole rotors and contribute to poor cooling of the central region of the rotor. On the experimental rotor the V-blocks covered 40% of the area of the side of the field coils. The whole of the bottom faces of the coils were exposed to the airflow.

The inlet air was supplied from an external fan via inlet guide vanes, see Fig. 2, to permit the investigation of the effects of varying swirl in the air approaching the rotor on the flow field and heat transfer. The stator end windings were simplified to form a set of planar loops in order to simplify the CFD meshing. The pressure drop across the simplified end windings and their volume were similar to those in a real machine.

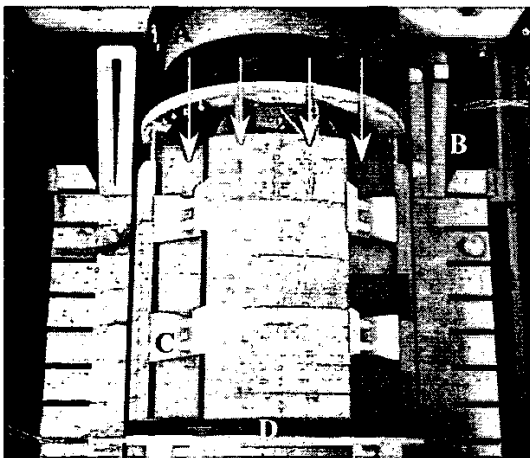


Fig. 2: Experimental rig with half of the stator removed, showing the inlet guide vanes (A), simplified end windings (B), V-blocks (C) in the rotor inter-polar spaces and the symmetry plane (D)

The rotor surface was hydraulically smooth as made. Heaters were embedded in the surface of one of the poles, providing heat fluxes typically between 1000 and 2000 W/m<sup>2</sup> and surface to air temperature differences between 10 and 20°C. The positions of 16 heat flux sensors, recording also the surface temperatures, are shown in Fig. 3.

The airflow was varied over the range from 0 to 1.3 m<sup>3</sup>/s. The rotor speed was limited to 900 rpm due to malfunctioning at higher speeds of the dataloggers recording data from sensors on the rotor. This equipment was housed in a chamber on the rotor shaft to avoid the need for multiple slipping connections.

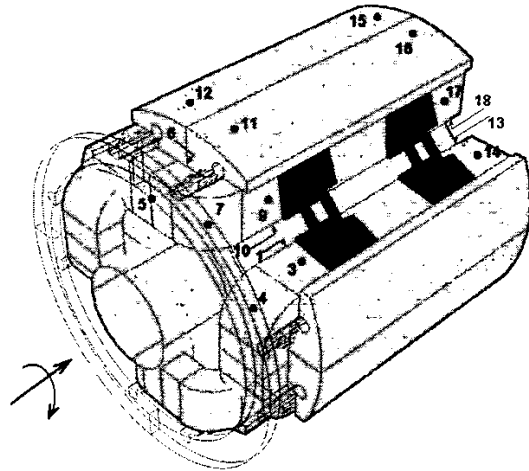


Fig. 3: Position of heat flux sensors on one rotor pole (positions 1,3,4,13 and 14 marked on another pole for clarity, points 1,10,13 and 18 were on centerlines of coil bottom faces)

#### CFD MODELLING

Around 2 million volume cells were typically employed in CFD models representative of the experimental arrangement described above. The commercial CFD code FLUENT5 was used for the analysis. The typical cell edge size was 3mm compared to the axial length of the model of 680 mm. Symmetry and 90° periodic boundary conditions were employed.

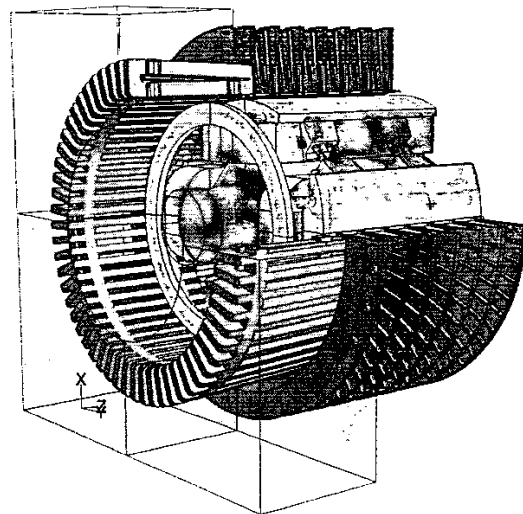


Fig. 4: CFD representation of the investigated machine, also showing contours of relative velocity on rotor.

For turbulence modelling, the standard k-ε model was used for its good convergence. The near-wall regions were treated by using the wall functions implemented in the CFD code. The Multiple Reference Frame approach for modelling rotor-stator interaction was used to obtain time-averaged steady state solutions. Small fluctuations in the flow field, such as those arising from the rotor passing individual teeth on stator bore could not, therefore, be modelled. A fully time-dependent solution

is feasible, but too demanding of processor time and memory.

A heat flux of  $1000\text{W/m}^2\text{K}$  on the rotor was applied locally, similarly to the position of heaters embedded in the surface of one experimental rotor pole with sensors on it. This was needed to avoid a rise in the bulk air temperature, since the inlet temperature was taken as the reference temperature for calculation of local heat transfer coefficients.

#### DISCUSSION OF RESULTS

Heat transfer coefficients were measured at 16 key locations around one rotor pole. Generally, the agreement of the experiments with the CFD predictions was good. In terms of absolute values, CFD tends to under-predict heat transfer coefficients by 20-30% if the Multiple Reference Frame approach for the rotor motion modelling is used. This is believed to be due to the steady state approximation of the rotor-stator interaction. The authors have previously shown (1) that this effect is mostly noticeable for surfaces near the interface between rotor and stator meshes, such as the pole top or the stator coils and teeth.

Good performance of CFD was also found in trend prediction. The response of the local heat transfer coefficients to the variation of three major parameters was studied. The parameters investigated were the air flow rate, rotor speed and the swirl angle. The axial inlet velocity of the cooling air  $v_{ax}$  varied between 3 and 15 m/s, the rotor tip velocity  $v_t$  varied between 11.8 and 22 m/s. Although the interpolar spaces had a smaller cross section area than the inlet, the inlet velocity corresponded to the velocity at the entry to the interpolar spaces due to a portion of air leaving through the finger ducts.

Over the range of parameters investigated, the increase with increased rotational speed of the heat transfer coefficient in the middle of the machine was stronger than that at the rotor entry. Similarly, increased axial flow affected the entry region more than the middle of the machine. This corresponds to the effects of the two parameters on the local velocity around the rotor.

No significant difference was recorded for the change of the air approach angle from 0 to  $55^\circ$ . This parameter was found to affect the flow distribution through stator ducts only slightly.

Figure 5 shows the response of measured and predicted heat transfer coefficients to the increase of flow rate at points 9 and 17 on the "leading" face of the rotor coil, see Fig.3. It was previously suggested (5) that the effect of flow rate becomes insignificant at a certain rotor speed. A similar effect can be seen in Fig.5; the heat transfer coefficients become dependent on flow rate when the ratio of axial inlet and rotor tip velocity exceeds 0.5.

For machines of the size of the experimental rig, the axial velocity at the entry to the inter-polar spaces could

occasionally reach more than 50% of rotor tip velocity. However, for larger machines, a ratio of axial inlet to rotor tip velocity around 0.3 or less is likely. In this context it could be assumed that the role of volumetric flow rate is to maintain sufficient surface-to-bulk air temperature difference, rather than to affect the heat transfer coefficients at low  $v_{ax}/v_{tip}$  ratios.

For the graphs shown, the points were chosen to show the typical difference in heat transfer coefficients at the ends of the rotor and in the middle of the machine. The level of heat transfer coefficients in the middle of the machine is around 40% of those at the rotor ends. The CFD predictions for the points in the middle of the machines were noticeably closer to experimental values. This could be explained by moderate flow conditions compared to the rotor entry.

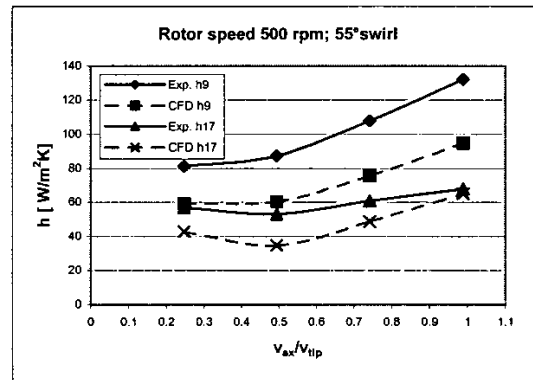


Fig. 5: Heat transfer coefficients at points 9 and 17 for variable airflow rate

Samples of responses of measured and predicted heat transfer coefficients to the change in rotor speed at two points on the "trailing" face of the rotor coil at two different flow rates are given in Fig. 6 and 7. The prediction of trends was again good, particularly for point 14, near the centre of the rotor.

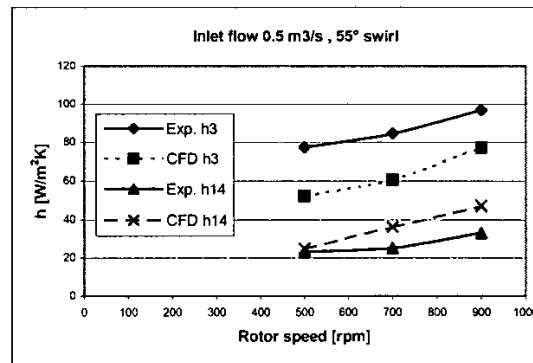


Fig. 6: Heat transfer coefficients at points 3 and 14 for variable rotor speed

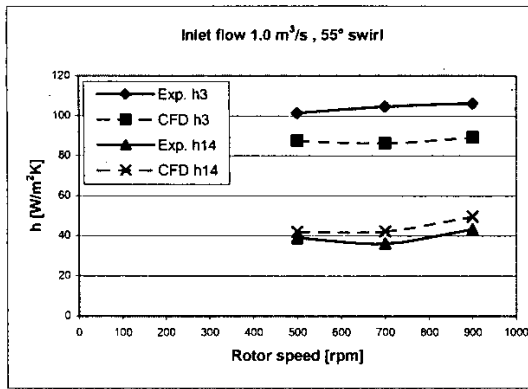


Fig. 7: Heat transfer coefficients at points 3 and 14 for variable rotor speed

Following validation, the CFD solutions provided much detailed information about the spatial distribution of heat transfer coefficients at flow conditions occurring in a real machine (Fig. 8).

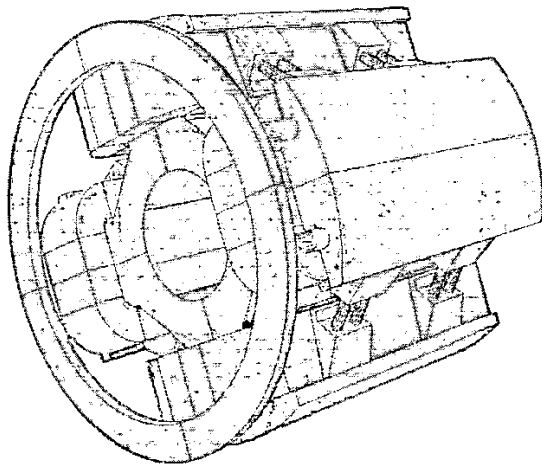


Fig. 8: Contours of heat transfer coefficients on a hydraulically smooth salient pole rotor

The highest heat transfer coefficients were predicted for the leading edge of the pole top, falling rapidly in the reverse rotation direction. Fig. 9 shows how the heat transfer coefficients on five selected lines on the surface of the 205mm wide pole top vary in the axial direction. The highest values are for points 5mm distant from the pole leading edge. Magnitudes are about double those for points along lines 50mm distant from the leading edge, centreline of the pole, points 50mm distant from the trailing edge and finally points 5mm distant from the trailing edge. The jumps present on these curves are associated with the rise of turbulence levels in areas of the air at entry to the stator radial ducts every 60 mm.

Based on experimental investigations it was previously suggested by Crew (4) that local heat transfer coefficients on rotors could be correlated with local velocity (measured by surface anemometer). In the present work, only some surfaces conformed to such a pattern, if the mean flow was reasonably aligned with

the surface. The coil bottom face on the leading side of the pole shows an example of such behaviour (Fig.10). But, on the coil bottom of the trailing side of the pole, the local velocity and heat transfer coefficients clearly contrast in behaviour (Fig.11).

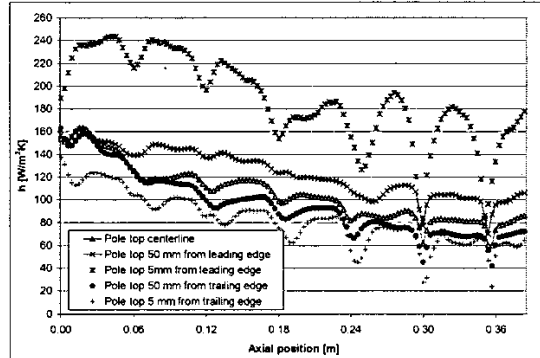


Fig. 9: Heat transfer coefficient on axial lines on the pole top

The CFD results indicated that the turbulence intensity was another factor influencing the magnitude of heat transfer coefficients in areas where the flow is swirling or forced to change direction around the geometry. In the current research no simple dependency of heat transfer coefficients on mean velocity magnitude could be confirmed for such surfaces.

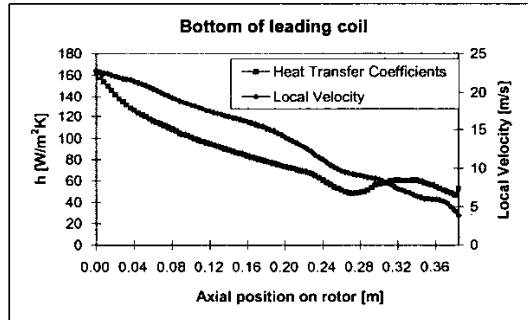


Fig. 10: Local velocity and surface heat transfer coefficients around bottom face of the field coil on leading side of pole

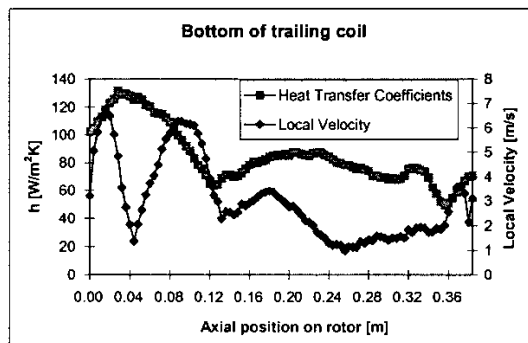


Fig. 11: Local velocity and surface heat transfer coefficients around bottom face of the field coil on trailing side of pole

### THE EFFECT OF V-BLOCKS ON THE FLOW AND HEAT TRANSFER

The coils on salient pole rotors are supported by V-blocks ensuring mechanical protection against centrifugal forces. The designs of V-blocks are various and they may also vary in the manner they occupy the inter-polar spaces.

In the present research several designs of V-blocks were examined with the intention of optimising their thermal performance through the use of CFD. In several instances, it was found that regions with very little flow developed close to the centre of the machine causing worsening of the cooling. This is in line with the finding that V-blocks tend to affect the heat transfer coefficients locally, rather than on the whole rotor.

Interestingly, for all types of V-blocks under investigation, the effect on the pressure drop through the machine was not as detrimental as might be expected. This is due to the stator being the dominant source of pressure drop in the machine.

### THE EFFECT OF SURFACE ROUGHNESS

Surface roughness is known to affect convective heat transfer significantly as it introduces disturbances into the viscous sublayer of boundary layers. The associated increased shear, however, increases ventilation loss. Modelling of many situations in the cooling of electrical machines requires a consideration of the potential of roughness or extended surfaces for enhancing the convection. In the present case, surface roughness effects need to be considered in interpreting measurements and predictions made for the smooth experimental model in the context of the rougher real machines surfaces.

The Wall Functions in the CFD code permit incorporation of the effect of roughness into the treatment of the near wall flow. The roughness is set by using two constants: roughness height,  $K_s$  and roughness constant,  $C_k$ .  $K_s$  is the equivalent sand grain height, if the roughness is uniform, or the  $D_{50}$  mean roughness diameter if it is not uniform.  $C_k$  is determined by the type of roughness. A value of 0.5 is normally used for uniform sand grain roughness.

The effect of surface roughness on the flow can be evaluated using the non-dimensional roughness height

$$K_s^+ = \frac{K_s * \rho * C_\mu^{0.25} * k^{0.5}}{\mu}$$

where  $k$  turbulent kinetic energy,  
 $\mu$  dynamic viscosity of air,  
 $\rho$  air density, and  
 $C_\mu$  dimensionless constant, in CFD modelling given by turbulence model (0.9)

According to the value of  $K_s^+$ , the flow regime is:

- ❖ Hydrodynamically smooth  $K_s^+ < 5$
- ❖ Transitional  $5 \leq K_s^+ \leq 70$
- ❖ Fully rough  $K_s^+ > 70$

A CFD case with roughness height  $K_s=1\text{mm}$  on all rotor surfaces was computed and compared to the case with smooth walls to illustrate the hypothetical enhancement of convection.

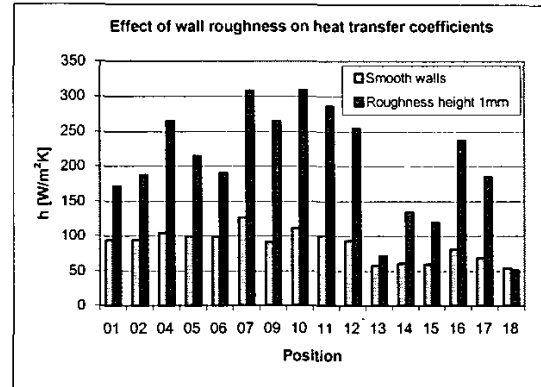


Fig. 12: The effect of the wall roughness on the heat transfer coefficients in positions on the rotor investigated

The value of  $K_s^+$  was calculated based on the CFD results for turbulent kinetic energy adjacent to rotor walls. The resulting value was 65, corresponding to the upper range of transitional regime.

The results of the comparison are shown in Fig. 12. Overall a 106% rise in the convective heat transfer was observed in the almost fully rough case when compared to the case with smooth surfaces. The modelled roughness also affected the pressure drop through the machine. Compared to the case with the smooth rotor, the predicted pressure drop rose by 22%.

### ACCOUNTING FOR EXTENDED TURNS OF COPPER ON SIDES OF COILS

Modelling some very fine geometrical details on rotor coils, such as extended turns of copper in strip-on-edge field coils was not feasible in the present 3D CFD models because of the grid density needed. Modelling the gap between two extended turns would require at least four cells across its width. The density of the grid used enabled modelling of the coil only with a flat surface.

The extended turns are an important feature influencing the amount of heat being dissipated from the coil by convection, especially as they are placed on the coil side towards which the heat is conducted in pure copper, with no intervening insulation. As a reasonable simplification, the ribbed surface was replaced by a surface with an equivalent roughness.

A sample of a ribbed heated surface was modelled in detail (Fig. 13) with typical dimensions for the width of the channels formed by the extended copper turns. Airflow with different approaching velocities was blown over this surface in three directions separately - parallel with the ribs, perpendicular to the ribs and at an angle of 45° to the ribs. It was found that the rate of

heat transfer computed from the ribs varied only by 15% when direction was changed from the cross-flow to the aligned flow. A further 10% increase was predicted for flow coming at an angle of 45°.

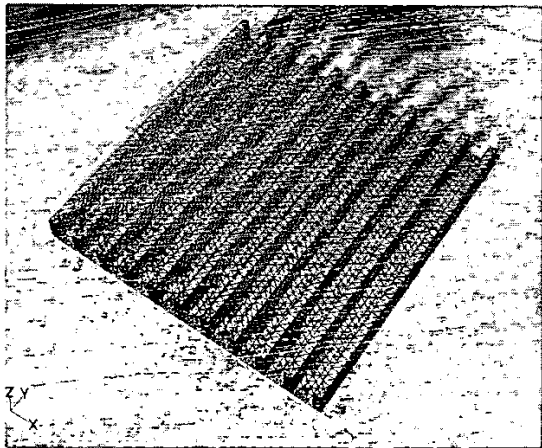


Fig. 13: Pathlines over ribbed surface coloured by velocity magnitude

The insensitivity of the ribbed surface roughness to the flow direction means that its replacement by a rough surface in the CFD model should not result in significant inaccuracies. The size of the equivalent sand grain roughness was set to provide an average heat transfer coefficient increased by a ratio based on the surface area with and without ribs in order to yield the same convective heat transfer. Such an exercise would need to be done individually for each design of extended turns to work out the appropriate value of equivalent sand grain roughness.

#### CONCLUSION

Experimental measurements provided data for validation of heat transfer coefficients predicted by CFD. The agreement was good both in terms of absolute values and the prediction of trends.

CFD was further shown to be a potential source of detailed information about the convective heat transfer taking place at operational conditions. The magnitude of heat transfer coefficients over the rotor was found to be very diverse, depending on a combination of at least two factors – the overall flow pattern and the intensity of turbulence.

The increases in heat transfer exhibited in a case with rough walls indicated the difference that might arise between the smooth experimental model and real motors and generators. They also indicate a possible route for enhancing heat transfer in some areas.

Until computational resources allow modelling of the very finest details, approximations such as the use of roughness to model extended turns on coils may be needed.

#### REFERENCES

1. Shanel M, Pickering SJ and Lampard D, 2000, "Application of Computational Fluid Dynamics to the Cooling of Salient Pole Electrical Machines", *Proc. of ICEM 2000*, Vol.1, 338-342
2. Pickering SJ, Lampard D and Shanel M, 2001, "Modelling Ventilation and Cooling of the Rotors of Salient Pole Machines", *Proc. of IEMDC*
3. Shanel M, Pickering SJ and Lampard D, 2001, "The Use of CFD for Thermal Optimisation of Large Air Cooled Salient Pole Electrical Machines", *Seminar on Selected Problems of Electric Machines and Drives*, Czech Republic
4. Carew NJ, 1992, "Experimental Determination of Heat Transfer Co-efficients of Salient Pole Rotors", *Thermal Aspects of Machines*, IEE, 1-8,
5. Liebe W., 1966, "Kühlung von Grossmaschinen", *ETZ-A*, vol. 87, No.13, 434-442

#### ACKNOWLEDGEMENTS

The authors would like to acknowledge the sponsors of this project - EPSRC and ALSTOM Electrical Machines, Ltd.